JMEPEG (2021) 30:3096–3106
https://doi.org/10.1007/s11665-021-05625-3

1059-9495/$19.00

Effect of Quasi-Continuous Equal-Channel Angular Pressing on Structure and Properties of Ti-Ni Shape Memory Alloys

R.D. Karelin, I.Yu. Khmelevskaya, V.S. Komarov, V.A. Andreev, M.M. Perkas, V.S. Yusupov, and S.D. Prokoshkin

Submitted: 5 November 2020 / Revised: 21 January 2021 / Accepted: 21 February 2021 / Published online: 19 March 2021

The effect of equal-channel angular pressing (ECAP) in quasi-continuous mode on the structure formation and mechanical and functional properties of a near-equiatomic Ti-Ni shape memory alloy (SMA) was studied in this work. ECAP with channel intersection angles of 110° and 120° was carried out at a temperature of 350-450 °C for 2-7 passes. Optimum deformation temperatures of ECAP in quasi-continuous mode are determined as 400 °C for ECAP with a channel intersection angle of 120° and 450 °C for 110°. ECAP with a channel intersection angle of 110° at a temperature of 450 °C yields high values of strength (yield stress σ_y = 1,090 MPa, ultimate tensile strength $\sigma_в$ = 1,150 MPa) and functional (maximum value of completely recoverable strain of 7.5% after ECAP and 8.4% after the addition of post-deformation annealing (PDA) at 400 °C for 1 h) characteristics. With the increase in the deformation temperature of quasi-continuous ECAP with a channel intersection angle of 110° from 350 to 450 °C, structure-morphological transformation in Ti-Ni SMA occurs. The shape of structural elements (grains and subgrains) changes from elongated to equiaxed; the size of the structural elements increases from less than 100 nm to 100-250 nm.

Keywords equal-channel angular pressing, nanostructure, severe plastic deformation, shape memory alloys, titanium nickelide, thermomechanical treatment

1. Introduction

The successful application of Ti-Ni-based shape memory alloys (SMAs) in various fields of engineering and medicine requires a rational combination of modern production technologies and methods of controlling functional characteristics, allowing one to fully implement the capabilities of these alloys (Ref 1-9). An increase in the combination of mechanical and functional properties of Ti-Ni SMA is associated with the formation of an ultrafine-grained (UFG) structure (Ref 10-14). For the formation of an UFG structure in various materials, a severe plastic deformation (SPD) is generally used (Ref 15-17). In the study (Ref 18), it was determined that the formation of a completely nanocrystalline structure provides the highest combination of mechanical and functional properties in Ti-Ni SMAs. These results were obtained on thin films, produced by a multi-pass cold rolling. Recently, in the study (Ref 19-21) the possibility of the formation a nanocrystalline structure in the bulk sample with the size of 1 cm^3 using MaxStrain deformation scheme was shown. However, for the industrial application of nanocrystalline Ti-Ni-based SMA the size of sample must be increased. Currently, one of the most promising methods for the formation of a UFG structure in bulk samples of various alloys, including SMA, is equal-channel angular pressing (ECAP) (Ref 22-27). According to (Ref 28, 29), after ECAP in a conventional mode with a channel intersection angle of 110° at deformation temperatures from 450 to 350 °C in 8-12 passes, generally, an equiaxial UFG submicrocrystalline structure of B2-austenite was formed in Ti-50.0-50.6 at %Ni SMA. The grain/subgrain size ranged from 200 to 300 nm, while in the initial recrystallized state before ECAP, the grain size was about 20 to 30 microns. The perspectives of application of ECAP in quasi-continuous mode (without pauses and the intermediate heating of the sample between passes) for obtaining bulk Ti-Ni SMA samples with a nanocrystalline structure were shown in (Ref 30). The application of quasi-continuous ECAP with a channel intersection angle of 120° at a temperature of 400 °C in seven passes allows the formation of a mixed nanograined and nanosubgrained structure with an average size of structural elements of 103±5 nm and increases the maximum completely recoverable strain up to 9.5%. In contrast, after the conventional ECAP mode (with pauses and the intermediate heating of the sample between passes) with a channel intersection angle of 120° at a temperature of 450 °C for twenty passes, only the submicrocrystalline structure with an average size of structural elements of 171±10 nm and a maximum completely recoverable strain of 7.2% was obtained (Ref 30). A schematic representation of the ECAP process in the quasi-continuous and conventional modes is shown in Fig. 1.

For the further expansion of possibilities of the quasi-continuous ECAP application, the effect of change of the main ECAP parameters, such as deformation temperature and strain, on the evolution of the structure and properties of Ti-Ni SMAs

R.D. Karelin and **V.S. Komarov**, National University of Science and Technology MISiS, Leninsky pr.4, Moscow 119 049, Russia; and Baikov Institute of Metallurgy and Materials Science, RAS, Leninsky pr.49, Moscow 119 334, Russia; **I. Yu. Khmelevskaya** and **S.D. Prokoshkin**, National University of Science and Technology MISiS, Leninsky pr.4, Moscow 119 049, Russia; and **V.A. Andreev, M.M. Perkas,** and **V.S. Yusupov**, Baikov Institute of Metallurgy and Materials Science, RAS, Leninsky pr.49, Moscow 119 334, Russia. Contact e-mail: rdkarelin@gmail.com.

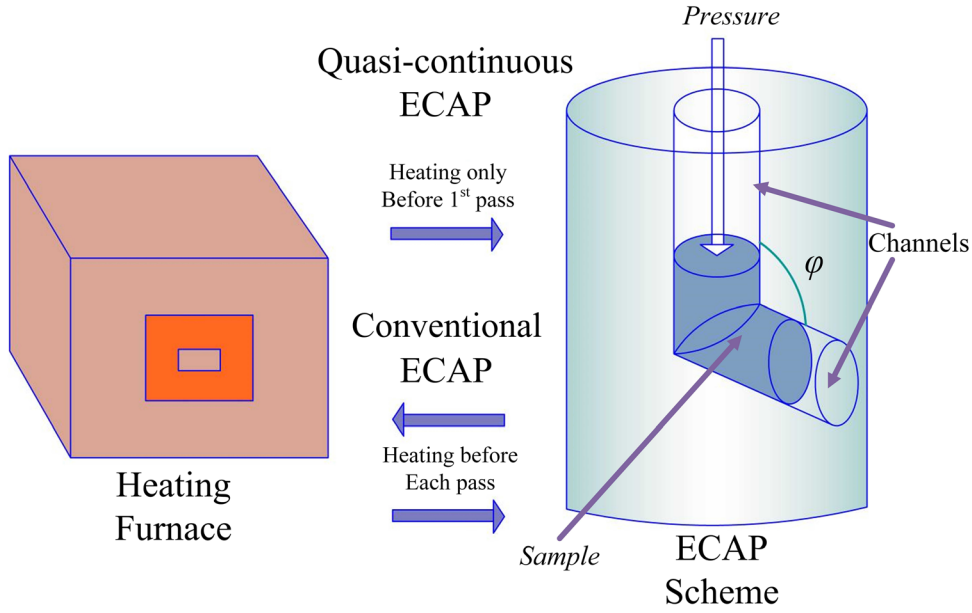

Fig. 1. Schematic representation of the ECAP process in quasi-continuous and conventional modes

must be studied. For this purpose, at the first stage of the work, to investigate the possibilities of additional structure refinement, a quasi-continuous ECAP mode with a channel intersection angle of 120° was used, and the deformation temperature was lowered from 400 to 350 °C. At the second stage, the possibility of the quasi-continuous ECAP application with a channel intersection angle of 110° and a temperature range of 350-450 °C was studied. This angle was chosen for the comparison with previous experience of the application of ECAP in conventional mode (Ref 28, 29).

Based on this information, the purpose of this work is defined as a comparative study of the cumulative effect of channel geometry, temperature, and strain degree on the evolution of the structure during ECAP in a quasi-continuous mode as well as the determination of the prospects of ECAP application for the formation of a completely nanocrystalline structure and the development of the highest possible combination of the mechanical and functional properties of Ti-Ni SMA.

2. Materials and Methods

A hot-rolled rod with a diameter of 20 mm and a length of 90 mm from near-equiatomic Ti-50.1 at.% Ni SMA, supplied by industrial center MATEK-SMA Ltd., was used as a billet for ECAP processing. The state of the sample after annealing at 750 °C for 30 min and cooling in water served as a reference treatment (RT) and was applied to all samples before ECAP (the starting temperature of forward martensitic transformation M_s = 38 °C). The accumulated true strain after ECAP was calculated using the following equation: $e = 2/\sqrt{3}\cdot ctg(\varphi/2)$, where φ is the channel intersection angle. The studied regimes of quasi-continuous ECAP and post-deformation annealing (PDA) are shown in Table 1.

Before the first ECAP pass, each sample was heated to the deformation temperature in the electric furnace chamber and then immediately transferred to the ECAP container, preliminarily heated to the required temperature that was maintained and controlled by the thermocouple placed on the depth of 4 cm from the container surface close to the matrix. Samples for all the applied research methods (Fig. 2) were cut from the workpiece after ECAP using the electrical erosion cutting machine as well as on a disk cutoff machine.

The samples for the determination of properties were polished and chemically pickled in an acid solution HF + HNO_3 + H_2O_2 with a ratio of 1:3:6 for removing the hardened layer. The samples for the TEM analysis were cut from the workpiece after ECAP at the half radius from the edge in perpendicular direction. Thin foil specimen for TEM analysis was obtained via the mechanical polishing of precut disks from 0.5-0.3 mm to 0.1 mm. Further disks were thinned via electrolytic polishing in an acid solution $HCLO_4$ + CH_3COOH.

After ECAP processing, PDA at a temperature of 400 °C for 1 h was applied. The application of PDA as a final operation of thermomechanical treatment (TMT) is justified, first, by the necessity to ensure the effectiveness of subsequent operations for inducing the required operational (“remembered”) shape and temperature range of shape recovery and, second, by the need to analyze the stability of the structure and properties obtained after TMT. The Vickers hardness measurements were carried out at room temperature using a *LECOM 400-A* tester under a load of 1 N and a dwell time of 10 sec. Not less than ten indentations were performed for each sample. The phase composition was studied using the *Ultima IV Rigaku* x-ray diffractometer in $Cu_{K\alpha}$ radiation in the 2Θ angle range from 35° to 47° at room temperature. An investigation of the microstructure was performed using a *JEM-2100* transmission electron microscope at an accelerating voltage of 200 kV. The mechanical properties were determined at room temperature by the uniaxial tensile tests using the universal tensile machine *INSTRON 3382* with a deformation rate of 2 mm/min. The obtained stress–strain diagrams were used to determine the following parameters: critical stress for martensite reorientation (or transformation yield stress) σ_{cr}, dislocation (conventional) yield stress σ_y, ultimate tensile strength σ_B, yield plateau strain ε_{pl}, difference between dislocation and transformation yield

Table 1. Studied regimes of quasi-continuous ECAP

No.	ECAP					Annealing	
	Temperature, °C	Number of passes	Accumulated true strain (*e*)	Channel intersection angle, °	Notation	Temperature, °C	Time, min
1	350	3	2.01	120	$ECAP3_{350}$	350, 400	60
2	380	4	2.68	120	$ECAP4_{380}$	350, 400	60
3	350	2	1.62	110	$ECAP2_{350}$	400	60
4	400	3	2.43	110	$ECAP3_{400}$	400	60
5	450	7	5.67	110	$ECAP7_{450}$	400	60

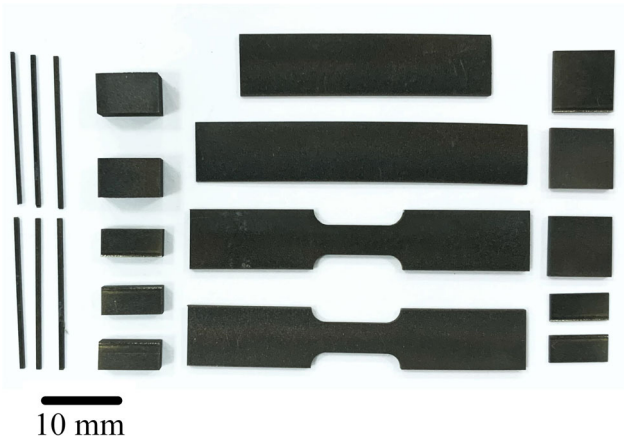

Fig. 2. Image of samples, cut from the workpiece after ECAP, for determination of mechanical and functional properties

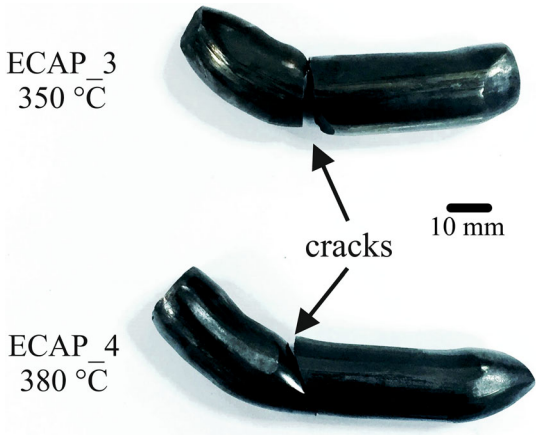

Fig. 3. Images of samples after ECAP at deformation temperatures of 350 °C and 380 °C with a channel intersection angle of 120° in three and four passes, respectively

stresses $\Delta\sigma = \sigma_y - \sigma_{cr}$, and relative elongation to failure δ. Characteristic temperatures of forward (start and finish temperatures M_s, M_f,) and reverse (start and finish temperatures A_s, A_f,) martensitic transformations were estimated by differential scanning calorimetry (DSC) method using a *Mettler-Toledo* calorimeter in the cooling-heating cycle at a rate of 10 K/min. Recoverable strain (ε_r) and maximum completely recoverable strain ($\varepsilon_{r,1}^{max}$) were estimated via a thermomechanical method using a bending mode for strain inducement. A detailed description of the thermomechanical method was provided in an earlier study (Ref 31). The error limits of the reported values are as follows: for σ ±15 MPa, for HV ±9, for δ ±1.4%, and for $\varepsilon_{r,1}^{max}$ ±0.3%.

3. Results and Discussion

3.1 The ECAP Procedure

Quasi-continuous ECAP with a channel intersection angle of 120° at lowered deformation temperatures, to 350 °C and 380 °C, allows only three and four passes to be carried out, respectively, with sample fragmentation in the last pass (Fig. 3). Previously, quasi-continuous ECAP was successfully conducted at a temperature of 400 °C for seven passes without sample damage (Ref 30). Sample destruction, after a comparatively small number of passes at a lowered deformation temperature, reveals the necessity of processing of quasi-continuous ECAP with a channel intersection angle of 120° at a temperature not lower than 400 °C.

The first application of quasi-continuous ECAP with a channel intersection angle of 110° was carried out at a temperature of 450 °C. Seven passes were successfully conducted without sample destruction. The eighth pass was not conducted because of the high probability of sample failure owing to the appearance of visible surface defects on the front end of the sample and, in addition, the considerable increase in pressure indication in the press hydraulic system. The lowering of the deformation temperature to 400 °C leads to crack formation during the third pass of quasi-continuous ECAP. At a deformation temperature of 350 °C, only two passes were carried out because of the high risk of the sample breaking during the next pass for the previously mentioned reasons. Images of the samples after ECAP in quasi-continuous mode with a channel intersection angle of 110° are shown in Fig. 4.

3.2 X-ray Diffraction Analysis

The results of x-ray diffraction analysis of the samples after various regimes of ECAP in quasi-continuous mode are presented as diffractogram excerpts in the 2Θ angle range—including the most intensive lines of B2-austenite, the intermediate rhombohedral R-phase, and monoclinic B19′-martensite—in Fig. 5.

After ECAP with φ = 120° both at 350 °C and 380 °C, x-ray lines of B19′-martensite and the R-phase are observed. Some amount of residual B2-austenite may be present, but

$\{110\}_{B2}$ austenite lines are not visualized clearly because of the overlapping of $\{330\}_R$ and $\{3\ \bar{3}0\}_R$ intermediate R-phase lines. PDA leads to the increase in the B19′-martensite amount. It should also be noted that after ECAP at 350 °C, the R-phase amount is much higher than that after ECAP at 380 °C.

X-ray diffraction analyses of the samples after ECAP with a channel intersection angle of 110° reveal that at room temperature, the x-ray lines of B19′-martensite, the intermediate R-phase, and B2-austenite are all present. The R-phase amount is higher than the amount of B19′-martensite compared to ECAP with $\varphi = 120°$ (Ref 30). This may be associated with the increase in deformation hardening and the corresponding increase in B2 → R transformation temperatures in conditions of a more rigid deformation regime. With the increased number of passes, the intensity of the R-phase lines also increases. Furthermore, after ECAP at 350 °C, a wider and unsplit peak of the R-phase indicates a lower degree of rhombohedricity (higher α angle) of the R-phase than after other studied regimes of ECAP. This, in turn, indirectly indicates a decrease in the temperature range of the forward martensitic transformation R → B19′ because of an increase in lattice defectness.

An evaluation of martensite x-ray line width after cooling to room temperature is extremely difficult because of its weak. Therefore, to compare lattice defectness after ECAP with different intersection angles, the martensite amount was increased via cooling in liquid nitrogen and reheating to room temperature (Fig. 4c). The results of the x-ray $(111)_{B19'}$ line width evaluation are shown in Table 2.

Based on the obtained results, despite an increase in the deformation temperature of 50 °C, the lattice distortion degree after ECAP7 with a channel intersection angle of 110° is higher than that after ECAP7 with a channel intersection angle of 120°. The decrease in the channel intersection angle from 120° to 110° and the associated increase in the true accumulated strain after one pass from $e = 0.67$ to $e = 0.81$ lead to an increase in lattice distortion and, from this point of view, allow the deformation temperature to increase from 400 to 450 °C with corresponding increase in deformation hardening.

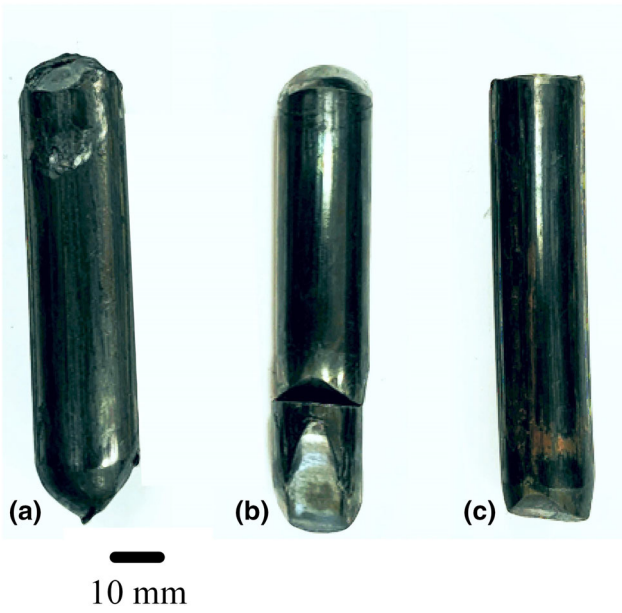

Fig. 4. Images of samples after ECAP in quasi-continuous mode with a channel intersection angle of 110°: $ECAP7_{450}$ (a), $ECAP3_{400}$ (b), and $ECAP2_{350}$ (c)

3.2.1 Transmission Electron Microscopy. An TEM study of the resultant structure and phase composition of the Ti-Ni near-equiatomic alloy was carried out after quasi-continuous ECAP with a channel intersection angle of 110° in a temperature range of 350-450°C. A structure analysis of the samples after ECAP with a channel intersection angle of 120° was not conducted since, as will be shown further, the obtained combination of mechanical and functional properties (especially maximum completely recoverable strain value) is lower compared with that previously studied (Ref 30) on the quasi-continuous ECAP regime in seven passes at a temperature of 400 °C. As a result, bright and dark field images and electron diffraction patterns were obtained, which are shown in Fig. 6, 7, 8.

Figure 6(a) and (b) shows the alloy structure obtained after quasi-continuous ECAP with a channel intersection angle of 110° at a deformation temperature of 350 °C in two passes ($e = 1.62$). The number of passes is determined by the appearance of clearly observed fracture zones (surface cracks) and the high probability of sample fragmentation during the next pass. An analysis of the bright and dark field images reveals deformation bands that are elongated perpendicularly to the sample axis.

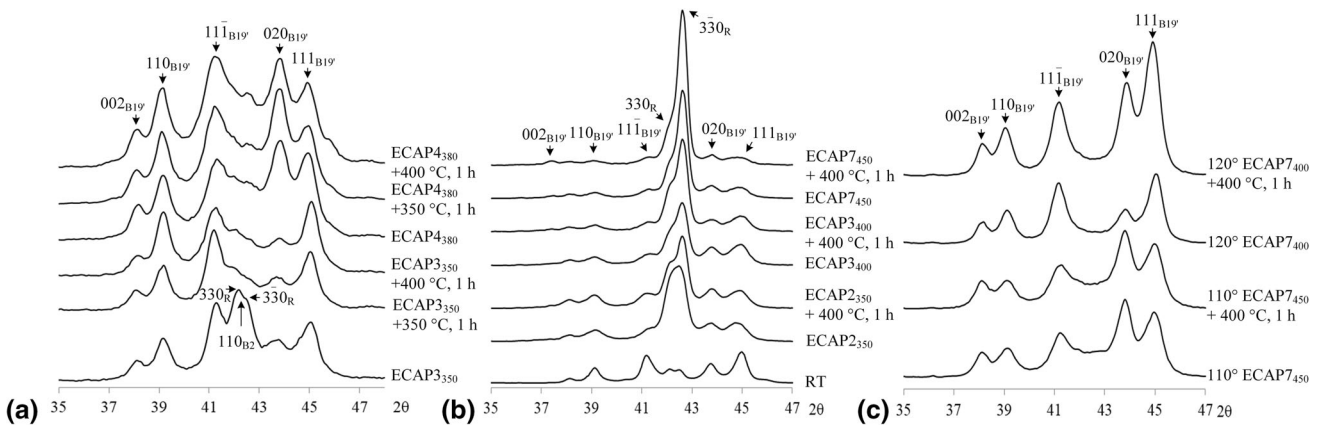

Fig. 5. X-ray diffractograms of Ti-Ni SMA after ECAP with channel intersection angle $\varphi = 120°$ at 350 °C and 380 °C and PDA at 350 °C and 400 °C, 1 h (a), after ECAP with $\varphi = 110°$ at 450 °C, 400 °C, and 350 °C and PDA at 400 °C, 1 h (b), and after ECAP7 with $\varphi = 110°$ and 120° at 450 °C and 400 °C, respectively, and PDA at 400 °C, 1 h, after cooling in liquid nitrogen (c)

Table 2. X-ray line $(111)_{B19'}$ width after various ECAP regimes measured after cooling in liquid nitrogen and reheating to RT

ECAP regimes	Channel intersection angle φ, °	B_{111} (°2θ)
RT	…	0.52±0.03
$ECAP7_{450}$	110	0.98±0.05
$ECAP7_{450}$ + 400 °C , 1 h	110	0.95±0.05
$ECAP7_{400}$	120	0.80±0.05
$ECAP7_{400}$ + 400 °C , 1 h	120	0.78±0.05

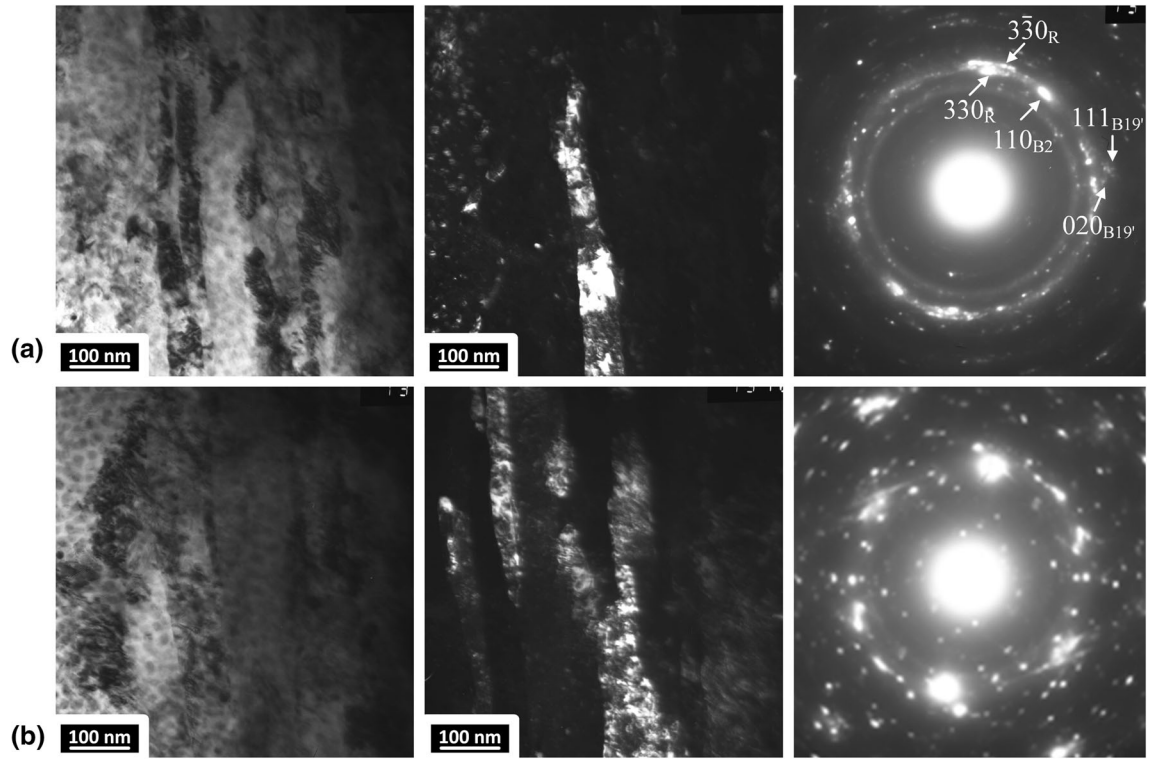

Fig. 6. Microstructure of Ti-Ni near-equiatomic SMA after ECAP with a channel intersection angle of 110° at 350 °C for two passes (a, b). Transmission electron microscopy: bright and dark field images and electron diffraction patterns

The deformation bands contain equiaxed and ellipsoidal structure elements; the main axis of the ellipsoidal structure elements is also perpendicular to the sample axis direction. Based on the dark field images, the deformation bands have an alternating crystallographic orientation and contain a developed dislocation substructure with a very high density of free (not involved in boundaries and subboundaries) dislocations ($\sim 10^{11}$ cm^{-2}). The average transverse size of the structural elements after ECAP with a channel intersection angle of 110° at a temperature of 350 °C for two passes is less than 100 nm. An analysis of the dark field images shows that these structure elements are subgrains (with low-angle misorientation) and grains (with high-angle misorientation). An analysis of the diffraction patterns reveals the existence of all three main phases in the sample after studied treatment: B2-austenite and B19′-, R-martensites. The representative reflections of these three phases are indicated in the electron diffraction pattern (Fig. 6a). The identification of the B2-phase in the electron diffraction pattern must be noted. In the x-ray diffraction patterns, this phase could not directly identified given the superimposition of x-ray lines of the R-phase on the lines of the B2-phase. In the electron diffraction pattern, the reflexes of these two phases are azimuthally shifted relative to each other and can be reliably identified despite the low radial resolution compared to the x-ray diffraction pattern. Electron diffraction patterns have an annular shape, typical for the formation of nanocrystalline structures. The relative position of individual reflections or groups of reflections of the one electron diffraction pattern ring indicates the presence of both low-angle and high-angle misorientations, thereby confirming the conclusion based on the analysis of the dark field images.

The increase in the deformation temperature of quasi-continuous ECAP to 400 °C decreases the deformation resistance and allows the true accumulated strain to increase to e = 2.43 by adding one more pass. An analysis of the corresponding electron micrograph images in Fig. 7 shows that the size of the structure elements distinctly increases and lies in the range from 50 nm to 150 nm. The elongation of grains/subgrains is

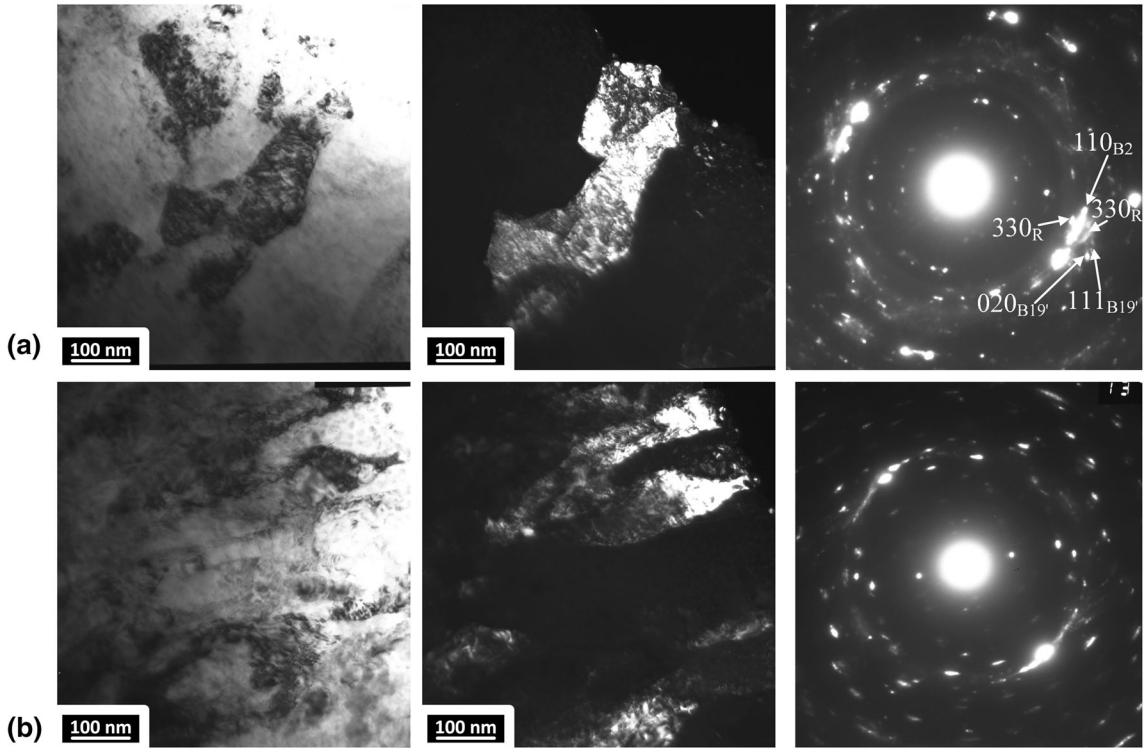

Fig. 7. Microstructure of Ti-Ni near-equiatomic SMA after ECAP with a channel intersection angle of 110° at 400 °C for three passes (a, b). Transmission electron microscopy: bright and dark field images and electron diffraction patterns

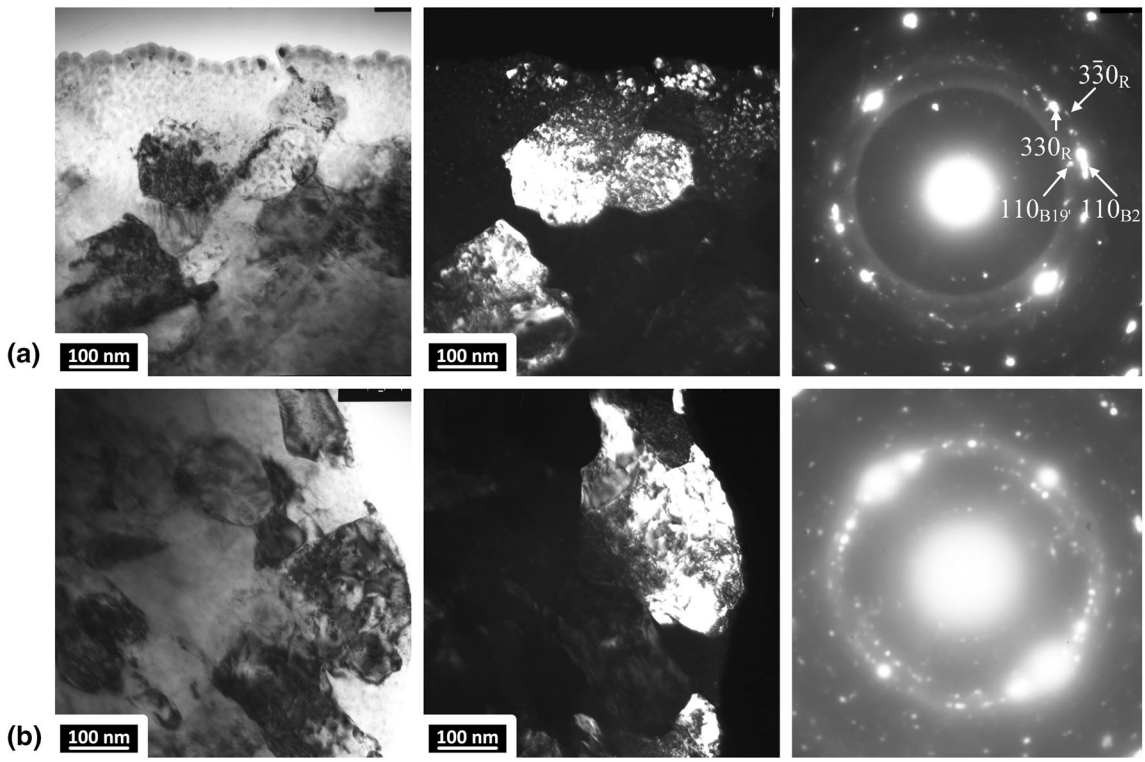

Fig. 8. Microstructure of Ti-Ni near-equiatomic SMA after ECAP with a channel intersection angle of 110° at 450 °C for seven passes (a, b). Transmission electron microscopy: bright and dark field images and electron diffraction patterns

maintained but less noticeable compared with those during deformation at 350 °C. The phase composition (B2-austenite and B19′-, R-martensites) is stable. The free dislocation density remains high. The annular shape of the electron diffraction patterns becomes less pronounced because of the decrease in the azimuthal smearing of the phase reflections, which indicates

a decrease in the local lattice distortion because of some decrease in its defect density.

An additional increase in the deformation temperature to 450 °C leads to the enhancement of ductility of the alloy; seven passes of ECAP with a channel intersection angle of 110° (e = 5.67) do not result in sample fragmentation. Applying this ECAP regime leads to the growth of structural elements to 100-250 nm and some decrease in dislocation density, i.e., to a general lowering of lattice defectness compared to previous treatments (Fig. 8). A transition from a mostly elongated grain/subgrain structure to a predominantly equiaxed structure is observed. The reflections of all three phases are identified in the electron diffraction patterns: B2-austenite and B19′-, R-martensite.

Thus, the electron microscopy analysis reveals that within the studied temperature-deformation conditions of quasi-continuous ECAP with a channel intersection angle of 110°, the determining factor with the strongest effect on morphology, the size of the structure elements, and the degree of lattice defectness is deformation temperature. The following results of the deformation temperature's effect on the structure formation in the near-equiatomic Ti-Ni alloy in conditions of quasi-continuous ECAP with a channel intersection angle of 110° are defined; with the increase in the deformation temperature from 350 to 450 °C, the morphology of the structure elements (grains and subgrains) changes from elongated to equiaxed, the size of the structure elements increases from less than 100 nm to 100-250 nm, and the free dislocation density decreases while remaining within the same order of magnitude.

3.3 Mechanical and Functional Properties

The results of the Vickers hardness tests after the ECAP regimes with channel intersection angles of 120° and 110° and PDA are shown in Fig. 9.

The hardness values after ECAP with φ = 120° in three and four passes at 350 °C and 380 °C, respectively, are lower than after ECAP at 400 °C in seven passes. After ECAP with φ = 110°, the maximum hardness value (254 HV) is obtained after ECAP in seven passes at 450 °C. However, this value is considerably lower compared with that after ECAP in seven passes with φ = 120° at 400 °C. Low hardness values after ECAP with φ = 110° are associated with changes in the phase composition of the alloy at room temperature. Measurements in the R-phase state near the starting temperature of forward martensitic transformation M_s reveal a decrease in hardness value given the increase of plasticity mechanism in the contribution of the stress-induced R → B19′ transformation mechanism to the overall deformation process. PDA at 400 °C for 1 h does not lead to a significant (more than 10 HV) decrease in hardness value after the studied ECAP regimes, which indicates the stability of the obtained structure.

DSC study shows that after RT, both forward and reverse martensitic transformations pass through one stage: B2 → B19′ and B19′ → B2, respectively (Fig. 10). Their characteristic transformation temperatures are as follows: M_s (start) = 40 °C, M_p (peak) = 32 °C, M_f (finish) = 24 °C for the forward MT, and A_s (start) = 52 °C, A_p (peak) = 67 °C, A_f (finish) = 72 °C for the reverse MT. The quasi-continuous ECAP entailed development of internal stress fields, which resulted in splitting of the direct MT into two stages: B2 → R and R → B19′, with following characteristic transformation temperatures: R_s (start) = 52 °C, R_p (peak) = 36 °C, R_f (finish) = 17 °C for the former, and M_s (start) = 24 °C, M_p (peak) = 2 °C, M_f (finish) = − 11 °C for the latter. Thus, a considerable lowering of the B19′-martensite formation temperatures is observed as well. The reverse MT range (A_s−A_f) slightly shifts toward lower temperatures after ECAP (A_s = 48 °C, A_p = 61 °C, A_f = 65 °C). The described changes in the MT kinetics correlate well with known results for severely deformed and annealed Ti-Ni alloys (Ref 19).

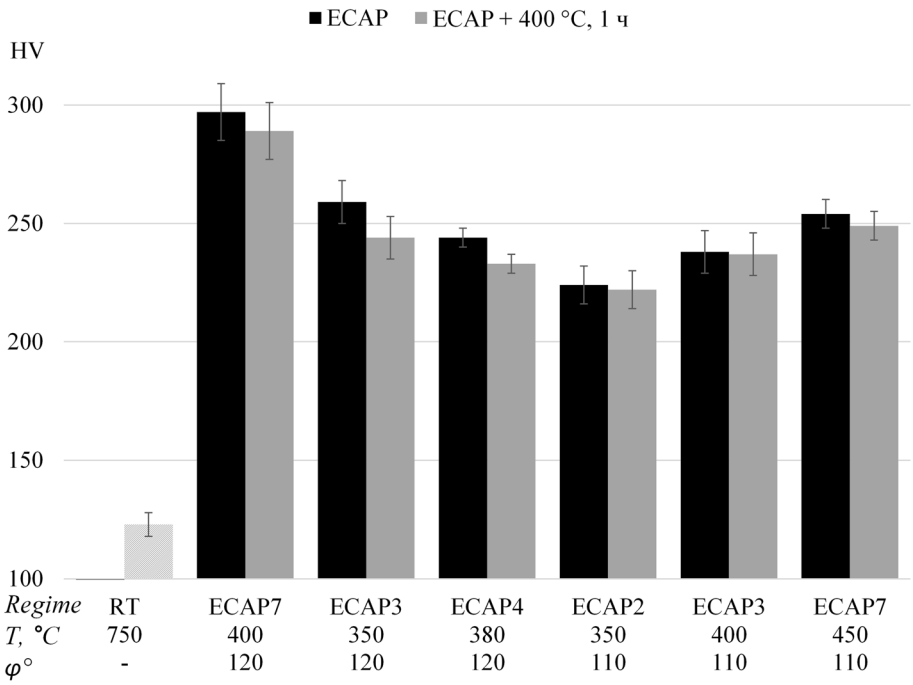

Fig. 9. Hardness test results after various ECAP regimes and after ECAP + PDA at 400 °C, 1 h

Representative stress–strain diagrams after ECAP with φ = 110° are shown in Fig. 11. The main stress and strain parameters σ_{cr}, σ_y, $\sigma_в$, ε_{pl}, $\Delta\sigma$, and δ are schematically shown in the inset to Fig. 11. The maximum completely recoverable strain versus the ECAP regimes is shown in Fig. 12. Based on the conducted research, a unifying Table 3 containing the mechanical and functional properties after all the studied ECAP regimes was compiled.

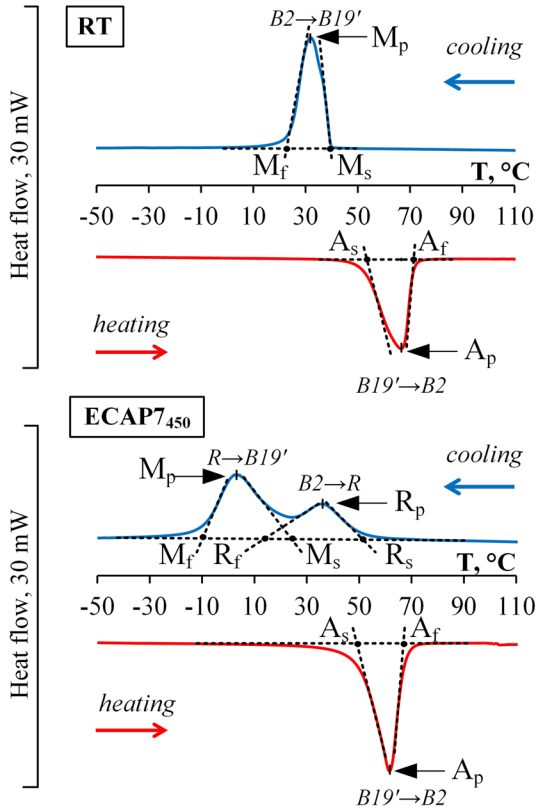

Fig. 10. Calorimetric curves of Ti-Ni near-equiatomic SMA after RT and ECAP7$_{450}$

The mechanical behavior of the samples during the tensile tests is typical for thermomechanically treated Ti-Ni near-equiatomic alloys with the structure of martensite and the R-phase. A less predominant inclined yield plateau is observed because of the development of R → B19′ transformation under the loading and reorientation of B19′-martensite. The strength characteristics after lowering the deformation temperature of quasi-continuous ECAP to 350 °C and 380 °C with φ = 120° are slightly lower (σ_y of 50 MPa in average, $\sigma_в$ of 100 MPa in average) compared with the results, obtained after ECAP at 400 °C in more passes (Ref 30). With the decrease in the channel intersection angle for all the studied ECAP regimes, an increase in the dislocation yield stress to 1000 MPa and higher is observed, which indicates an increase in deformation hardening (Table 3). In the case of the identical regime for both variants of the channel intersection angle of ECAP3$_{400}$, σ_y equals 1000 MPa for φ = 110° against 855 MPa for φ = 120° (Ref 30). The critical stress for martensite reorientation σ_{cr}, which is determined by the position of the deformation temperature relative to the temperature M_s, in the case of φ = 110°, has lower values of 90-150 MPa. Abnormally high plasticity of δ = 50-70% is a consequence of premartensitic softening (Ref 32-35) because, as shown by the x-ray analysis (Fig. 5), deformation at room temperature occurs in the presence of the R-phase.

The highest value of $\Delta\sigma$, which substantially determines a resource of maximum completely recoverable strain (Ref 36), for φ = 110°, is 1,010 MPa after seven passes of ECAP and PDA at 400 °C, 1 h. This is confirmed by the maximum value of completely recoverable strain of 8.4% obtained after this TMT regime. PDA at 400 °C leads to the increase in recoverable strain given the lowering of the transformation yield stress while retaining a high value of dislocation yield stress and a corresponding increase in $\Delta\sigma$. The maximum

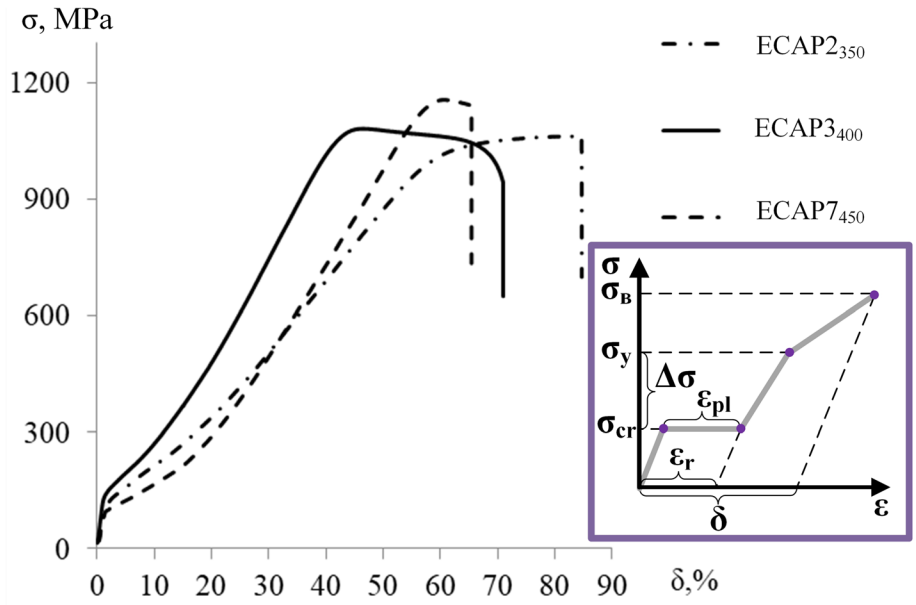

Fig. 11. Typical tensile diagrams of Ti-Ni near-equiatomic SMA after ECAP with a channel intersection angle of 110° at 350, 400, and 450 °C for two, three, and seven passes, respectively

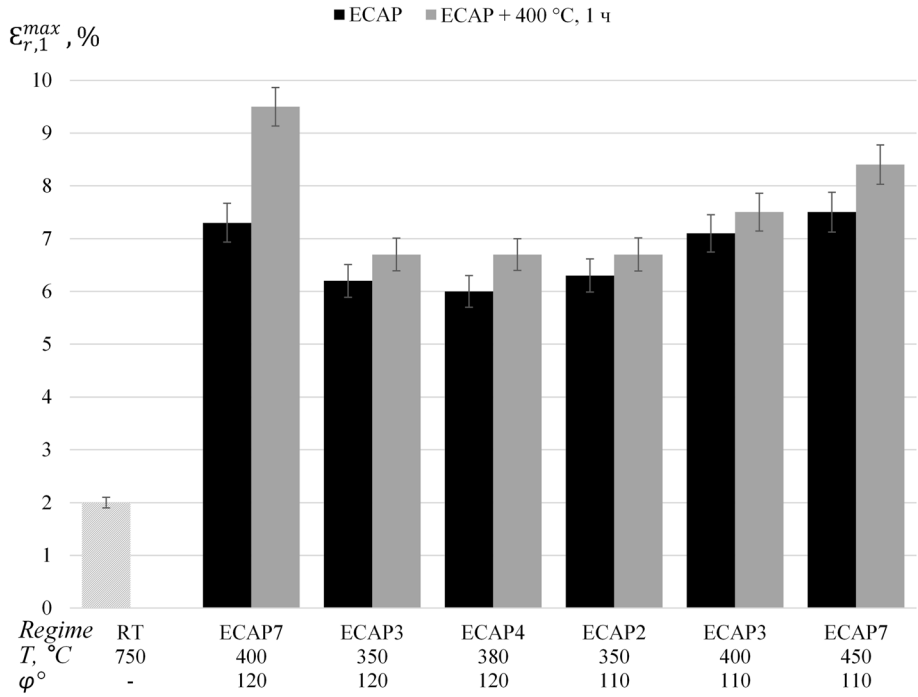

Fig. 12. Maximum completely recoverable strain of Ti-Ni near-equiatomic SMA after various ECAP regimes and PDA

Table 3. Mechanical and functional properties of Ti-Ni near-equiatomic SMA after various ECAP regimes

ECAP regime	σ_{cr}, MPa	σ_y, MPa	$\Delta\sigma$, MPa	$\sigma_в$, MPa	δ, %	HV, ea	$\varepsilon_{r,1}^{max}$, %
RT	100	430	330	700	28	176	2.0
$ECAP3_{350}120$	170	900	730	1024	30	259	6.2
$ECAP3_{350}120$ + 400 °C , 1 h	140	910	810	1018	25	244	6.7
$ECAP4_{380}120$	150	915	750	1052	38	244	6
$ECAP4_{380}120$ + 400 °C , 1 h	100	900	800	1035	37	233	6.7
$ECAP2_{350}110$	125	870	745	1060	69	224	6.3
$ECAP2_{350}110$ + 400 °C , 1 h	100	950	850	1070	70	222	6.7
$ECAP3_{400}110$	150	1000	850	1020	52	238	7.1
$ECAP3_{400}110$ + 400 °C , 1 h	120	1000	880	1050	49	237	7.5
$ECAP7_{450}110$	100	1090	990	1150	50	254	7.5
$ECAP7_{450}110$ + 400 °C , 1 h	90	1100	1010	1200	49	249	8.4

completely recoverable strain after lowering the temperature of quasi-continuous ECAP with φ = 120° to 350 and 380 °C and PDA at 400 °C, 1 h, is noticeably lower compared with ECAP at 400 °C and PDA at 400 °C, 1 h, in more passes (6.7% against 9.5%), which confirms insufficient structure refinement because of sample fragmentation after quasi-continuous ECAP at lowered deformation temperatures.

An analysis of the deformation parameters, structure, and properties of Ti-Ni near-equiatomic alloy after ECAP in quasi-continuous mode allows one to conclude that for the production of a defect free sample and the accumulation of a sufficient strain with a decrease in the channel intersection angle to 110°, it is reasonable to conduct ECAP at a temperature higher than 400 °C, more specifically at 450 °C. To obtain bulk nanostructured semi-finished products of Ti-Ni SMA with improved mechanical and functional properties, the most promising regimes of TMT are quasi-continuous ECAP with channel intersection angles of 120° and 110° in five to seven passes at temperatures of 400 °C and 450 °C, respectively. ECAP with a channel intersection angle of 110° allows one to obtain higher values of strength characteristics and, after ECAP with a channel intersection angle of 120°, a more uniform structure, providing the highest value of completely recoverable strain of 9.5% after PDA is formed.

4. Conclusions

1. A comparative study of the effect of various technological parameters of ECAP on the structure and properties of Ti-Ni SMA confirms the advantage of the quasi-continuous ECAP application for the formation of a nanocrystalline structure and a considerable improvement of mechanical and functional characteristics and reveals

optimum deformation temperatures as 400 °C for ECAP with a channel intersection angle of 120° and 450 °C for 110°. ECAP at a temperature lower than 400 °C leads to premature sample fragmentation and does not provide the improvement of properties compared with ECAP at a higher deformation temperature for more passes.

2. TEM study after quasi-continuous ECAP with a channel intersection angle of 110° reveals that the deformation temperature is a key factor affecting morphology, average size of structure elements (grains and subgrains), and degree of lattice defectness. The size of the structure elements increases from less than 100 to 100-250 nm, and the dislocation density decreases, although remaining within the same order of magnitude, as the deformation temperature of quasi-continuous ECAP with a channel intersection angle of 110° increases from 350 to 450 °C.
3. A mixed nanograined and submicrocrystalline structure with high free dislocation density was formed in the bulk sample of Ti-Ni near-equiatomic SMA after quasi-continuous ECAP with a channel intersection angle of 110° in seven passes at 450 °C. This structure provides the best combination of mechanical and shape recovery properties as compared to the reference treatment (RT): ultimate tensile strength of 1,150 MPa, completely recoverable strain of 7.5% versus 700 MPa and 2.0% after the RT.
4. The use of post-deformation annealing (PDA) at the deformation temperature after ECAP as a final stage of the thermomechanical treatment (TMT) eliminates excessive deformation hardening, does not change the size of the structural elements, and thus positively affects the structure and functional properties of near-equiatomic Ti-Ni SMAs: completely recoverable strain increases from 7.5 to 8.4%.
5. The most promising regimes of TMT for obtaining Ti-Ni SMA with mixed grained/subgrained close to nanoscale structure and improved mechanical and functional properties are quasi-continuous ECAP with channel intersection angle from 110° to 120° in five to seven passes at a temperature range of 400-450 °C.

Acknowledgments

The work was carried out with the support of the Ministry of Science and Higher Education of the Russian Federation in the framework of the State Task (project code 0718-2020-0030).

References

1. V. Brailovski, S.D. Prokoshkin, P. Terriault, F. Trochu, *Shape Memory Alloys: Fundamentals, Modeling and Applications*, Monreal: ETS Publishing, 2003, 851 p, https://espace2.etsmtl.ca/id/eprint/3754
2. J.M. Jani, M. Leary, A. Subic and M.A. Gibson, A Review of Shape Memory Alloy Research, Applications and Opportunities, *Mater. Des.*, 2014, **56**, p 1078–1113. https://doi.org/10.1016/j.matdes.2013.11.084
3. N. Resnina and V. Rubanik, *Shape Memory Alloys: Properties, Technologies, Opportunities*, Trans. Tech. Publications, Praffikon, 2015, p 640
4. Q. Sun, R. Matsui, K. Takeda, E. Pieczyska, Advances in Shape Memory Materials: In *Commemoration of the Retirement of Professor Hisaaki Tobushi*. New York: Springer, 2017, 73, 241 p, https://doi.org/https://doi.org/10.1007/978-3-319-53306-3
5. Z. Zeng, B.Q. Cong, J.P. Oliveira, W.C. Ke, N. Schell, B. Peng, Z.W. Qi, F.G. Gea, W. Zhange and S.S. Ao, Wire and Arc Additive Manufacturing of a Ni-Rich NiTi Shape Memory Alloy: Microstructure and Mechanical Properties, *Addit. Manuf.*, 2020, **32**, p 101051. https://doi.org/10.1016/j.addma.2020.101051
6. J.P. Oliveira, D. Barbosa, F.B. Fernandes and R.M. Miranda, Tungsten Inert Gas (TIG) Welding of Ni-Rich NiTi Plates: Functional Behavior, *Smart Mater. Struct.*, 2016, **25**(3), p 03LT01. https://doi.org/10.1088/0964-1726/25/3/03LT01
7. J.P. Oliveira, A.J. Cavaleiro, N. Schell, A. Stark, R.M. Miranda, J.L. Ocana and F.M. Braz Fernandes, Effects of Laser Processing on the Transformation Characteristics of NiTi: A Contribute to Additive Manufacturing, *Scripta Mater.*, 2018, **152**, p 122–126. https://doi.org/10.1016/j.scriptamat.2018.04.024
8. K.A. Polyakova, E.P. Ryklina and S.D. Prokoshkin, Effect of Grain Size and Ageing-Induced Microstructure on Functional Characteristics of a Ti-507 at% Ni Alloy, *Shape Memory and Superelasticity*, 2020, **6**, p 139–147. https://doi.org/10.1007/s40830-020-00269-z
9. E.P. Ryklina, K.A. Polyakova, NYu. Tabachkova, N.N. Resnina and S.D. Prokoshkin, Effect of B2 Austenite Grain Size and Aging Time on Microstructure and Transformation Behavior of Thermomechanically Treated Titanium Nickelide, *J. Alloys Compd.*, 2018, **764**, p 626–638. https://doi.org/10.1016/j.jallcom.2018.06.102
10. D. Gunderov, A. Churakova, A. Lukyanov, E. Prokofiev, V. Pushin, A. Kreitcberg and S. Prokoshkin, Features of the Mechanical Behavior of Ultrafine-Grained and Nanostructured TiNi Alloys, *Mater. Today: Proc.*, 2017, **4**(3), p 4825–4829. https://doi.org/10.1016/j.matpr.2017.04.078
11. I. Khmelevskaya, V. Komarov, R. Kawalla, S. Prokoshkin and G. Korpala, Effect of Biaxial Isothermal Quasi-Continuous Deformation on Structure and Shape Memory Properties of Ti-Ni Alloys, *J. Mater. Eng. Perform*, 2017, **26**(8), p 4011–4019. https://doi.org/10.1007/s11665-017-2841-1
12. S. Prokoshkin, I. Khmelevskaya, V. Andreev, R. Karelin, V. Komarov and A. Kazakbiev, Manufacturing of Long-Length Rods of Ultrafine-Grained Ti-Ni Shape Memory Alloys, *Mater. Sci. Forum*, 2018, **918**, p 71–76
13. A.A. Churakova and D.V. Gunderov, Microstructure and Mechanical Properties of the Ultrafine-Grained TiNi Alloy After Multiple Martensitic Transformations and Subsequent Aging, *IOP Conf. Ser. Mater. Sci. Eng*, 2019 https://doi.org/10.1088/1757-899X/672/1/012025
14. V. Komarov, I. Khmelevskaya, R. Karelin, R. Kawalla, G. Korpala, U. Prahl, V. Yusupov and S. Prokoshkin, Deformation Behavior, Structure, and Properties of an Aging Ti-Ni Shape Memory Alloy after Compression Deformation in a Wide Temperature Range, *JOM*, 2021 https://doi.org/10.1007/s11837-020-04508-7
15. R.Z. Valiev, A.V. Korznikov and R.R. Mulyukov, Structure and Properties of Ultrafine-Grained Materials Produced by Severe Plastic Deformation, *Mater. Sci. Eng. A.*, 1993, **168**(2), p 141–148. https://doi.org/10.1016/0921-5093(93)90717-S
16. R. Valiev, Y. Estrin, Z. Horita, T. Langdon, M. Zehetbauer and Y. Zhu, Producing Bulk Ultrafine-Grained Materials by Severe Plastic Deformation, *JOM*, 2006, **58**, p 33–39. https://doi.org/10.1007/s11837-006-0213-7
17. I. Sabirov, N. Enikeev, M. Murashkin, R. Valiev, *Bulk Nanostructured Materials with Multifunctional Properties*, New York: Springer, 2015, 118 p, https://doi.org/https://doi.org/10.1007/978-3-319-19599-5
18. V. Brailovski, S. Prokoshkin, I. Khmelevskaya, K. Inaekyan, V. Demers, S. Dobatkin and E. Tatyanin, Structure and Properties of the Ti-500 at% Ni Alloy After Strain Hardening and Nanocrystallizing, *Mater. Trans*, 2006 https://doi.org/10.2320/matertrans.47.795
19. V. Komarov, I. Khmelevskaya, R. Karelin, S. Prokoshkin, M. Zaripova, M. Isaenkova, G. Korpala and R. Kawalla, Effect of Biaxial Cyclic Severe Deformation on Structure and Properties of Ti-Ni Alloys, *J. Alloys Compd*, 2019, **797**, p 842–848. https://doi.org/10.1016/j.jallcom.2019.05.127
20. IYu. Khmelevskaya, R. Kawalla, S.D. Prokoshkin and V.S. Komarov, Effect of Multiaxial Deformation Max-Strain on the Structure and Properties of Ti-Ni Alloy, *IOP Conf. Ser. Mater. Sci. Eng.*, 2014, **63**, p 012108. https://doi.org/10.1088/1757-899X/63/1/012108

21. I. Khmelevskaya, V. Komarov, R. Kawalla, S. Prokoshkin and G. Korpala, Features of Ti-Ni Alloy Structure Formation Under Multi-Axial Quasi-Continuous Deformation and Post-Deformation Annealing, *Mater. Today: Proc.*, 2017, **4**(3), p 4830–4835. https://doi.org/10.1016/j.matpr.2017.04.079
22. R.Z. Valiev and T.G. Langdon, Principles of Equal-Channel Angular Pressing as a Processing Tool for Grain Refinement, *Prog. Mater Sci.*, 2006, **51**, p 881–981. https://doi.org/10.1016/j.pmatsci.2006.02.003
23. H. Shahmir, M. Nili-Ahmadabadi, M. Mansouri-Arani and T.G. Langdon, The Processing of NiTi Shape Memory Alloys by Equal-Channel Angular Pressing at Room Temperature, *Mater. Sci. Eng. A.*, 2013, **576**, p 178–184. https://doi.org/10.1016/j.msea.2013.04.001
24. IYu. Khmelevskaya, R.D. Karelin, S.D. Prokoshkin, M.G. Isaenkova, Yu.A. Perlovich, V.A. Fesenko, V.S. Komarov and M.M. Zaripova, Features of Nanostructure and Functional Properties Formation in Ti-Ni Shape Memory Alloys Subjected to Quasi-Continuous Equal Channel Angular Pressing, *IOP Conf. Ser. Mater. Sci. Eng*, 2019 https://doi.org/10.1088/1757-899X/503/1/012024
25. G. Raab, The Innovation Potential of ECAP Techniques of Severe Plastic Deformation, *IOP Conf Ser. Mater. Sci. Eng*, 2014 https://doi.org/10.1088/1757-899X/63/1/012009
26. S.N. Lezhnev, I.E. Volokitina and D.V. Kuis, Evolution of Microstructure and Mechanical Properties of Composite Aluminum-Based Alloy during ECAP, *Phys. Met. Metallogr.*, 2018, **119**(8), p 810–815. https://doi.org/10.1134/S0031918X18040129
27. V.G. Pushin, R.Z. Valiev, Y.T. Zhu, S.D. Prokoshkin, D.V. Gunderov and L.I. Yurchenko, Effect of Equal-Channel Angular Pressing and Repeated Rolling on Structure Phase Transformations and Properties of TiNi Shape Memory Alloys, *Mater. Sci. Forum*, 2006, **503–504**, p 539–544
28. IYu. Khmelevskaya, S.D. Prokoshkin, I.B. Trubitsyna, M.N. Belousov, S.V. Dobatkin, E.V. Tatyanin, A.V. Korotitskiy, V. Brailovski, V.V. Stolyarov and E.A. Prokofiev, Structure and Properties of Ti–Ni-Based Alloys After Equal-Channel Angular Pressing and High-Pressure Torsion, *Mater. Sci. Eng. A*, 2008, **481–482**, p 119–122. https://doi.org/10.1016/j.msea.2007.02.157
29. V.V. Stolyarov, E.A. Prokofyev, S.D. Prokoshkin, S.V. Dobatkin, I.B. Trubitsyina, I.Y. Khmelevskaya, V.G. Pushin and R.Z. Valiev, Structure Features, Mechanical Properties and Shape Memory Effect in Ti-Ni Alloy, Processed by ECAP, *Phys. Met. Metallogr*, 2005, **100**, p 608–618
30. IYu. Khmelevskaya, R.D. Karelin, S.D. Prokoshkin, V.A. Andreev, V.S. Yusupov, M.M. Perkas, V.V. Prosvirnin, A.E. Shelest and V.S. Komarov, Effect of the Quasi-Continuous Equal-Channel Angular Pressing on the Structure and Functional Properties of Ti-Ni-Based Shape-Memory Alloys, *Phys. Met. Metallogr*, 2017, **118**, p 279–287. https://doi.org/10.1134/S0031918X17030073
31. H.C. Lin and S.K. Wu, Strengthening Effect on Shape Recovery Characteristic of the Equiatomic TiNi Alloy, *Scripta Metall. Mater*, 1992, **26**, p 59–62. https://doi.org/10.1016/0956-716X(92)90369-P
32. V.G. Pushin, A.I. Lotkov, Y.R. Kolobov, R.Z. Valiev, E.F. Dudarev, N.N. Kuranova, A.P. Dyupin, D.V. Gunderov and G.P. Bakach, On the Nature of Anomalously High Plasticity of High-Strength Titanium Nickelide Alloys with Shape-Memory Effects: I. Initial Structure and Mechanical Properties, *Phys. Met. Metallogr*, 2008, **106**(5), p 520–530. https://doi.org/10.1134/S0031918X08110124
33. E.F. Dudarev, R.Z. Valiev, Yu.R. Kolobov, A.I. Lotkov, V.G. Pushin, G.P. Bakach, D.V. Gunderov, A.P. Dyupin and N.N. Kuranova, On the Nature of Anomalously High Plasticity of High-Strength Titanium Nickelide Alloys with Shape-Memory Effects: II. Mechanisms of Plastic Deformation Upon Isothermal Loading, *Phys. Met. Metallogr*, 2009, **107**(3), p 298–311. https://doi.org/10.1134/S0031918X09030120
34. E.P. Ryklina, S.D. Prokoshkin and A.A. Chernavina, Peculiarities of Implementation of Abnormally High Shape Memory Effects in Thermomechanically Treated Ti-Ni Alloys, *Inorg. Mater. Appl. Res.*, 2013, **4**(4), p 348–355. https://doi.org/10.1134/S2075113313040096
35. E. Ryklina, S. Prokoshkin and A. Kreytsberg, Abnormally High Recovery Strain in Ti–Ni-Based Shape Memory Alloys, *J. Alloys Compd.*, 2013, **577**(1), p 255–258. https://doi.org/10.1016/j.jallcom.2012.02.138
36. S. Prokoshkin, V. Brailovski, K. Inaekyan, V. Demers, I. Khmelevskaya, S. Dobatkin and E. Tatyanin, Structure and Properties of Severely Cold-Rolled and Annealed Ti-Ni Shape Memory Alloys, *Mater. Sci. Eng. A.*, 2008, **481–482**, p 114–118. https://doi.org/10.1016/j.msea.2007.02.150